Is Ambient Noise Tomography Across Ocean Basins Possible?

Fan-Chi Lin[1], Michael H. Ritzwoller[1], and Nikolai M. Shapiro[2]

1 – Center for Imaging the Earth's Interior, Department of Physics, University of Colorado at Boulder, Boulder, CO 80309-0390 USA,

linf@ciei.colorado.edu, (303 492 0985)

2 – Institut de Physique du Globe, Paris, France

Abstract

Based on year-long cross-correlations of broad-band seismic records obtained at sixty-six stations within or adjacent to the Pacific Basin, we show that broad-band ambient noise is observed to propagate coherently between island stations and between island and continent stations. For many station pairs, high signal-to-noise ratio (SNR) fundamental mode Rayleigh wave Green functions are observed, which establishes the physical basis for ambient noise tomography across the Pacific. Similar trends for continental and oceanic stations are observed in the relationship between the ambient noise level at a station and the “noise coherence distance” – the longest distance at which a high SNR cross-correlation signal is observed for a station. Because locally generated noise obscures long distance coherent noise, situating stations at quiet locations on islands is necessary for the success of ambient noise tomography. Local noise poses a particular challenge at atoll sites and, on the basis of analysis of data from station H2O, at ocean bottom sites at periods above ~25 sec. Reducing long-period (> 20 sec) local noise caused by tilts and subsurface deformation on ocean bottom stations by using horizontal components and differential pressure meters is recommended to improve the suitability of ocean bottom stations for ambient noise tomography.

Introduction

On continents around the globe ambient seismic noise has been shown to contain a significant component of broad-band Rayleigh wave energy extending from periods of several seconds to well in excess of 150 sec (e.g., Shapiro and Campillo, 2004). This noise is coherent over long distances and has proven useful to estimate fundamental mode Rayleigh wave Green functions by cross-correlating long noise sequences. Surface wave dispersion is measurable on these records and dispersion maps have been constructed on a variety of length scales and period bands in North America, Europe, and Asia (e.g., Shapiro et al., 2005; Sabra et al., 2005).

The present study addresses whether Rayleigh wave Green functions between pairs of oceanic stations or between continental and oceanic stations can be obtained using the same method. The question reduces to whether noise observed at ocean seismic stations is coherent over long distances, as it is in continental regions. This relates to the partitioning of ambient noise between noise generated near to the ocean station and noise generated further from the station that is coherent between distant stations. Determining the existence of coherent noise between pairs of stations is based on the observability of high signal-to-noise ratio (SNR) Green functions. If such Green functions are observed, then surface wave dispersion can be measured which will, ultimately, prove useful in the context of tomography. Tomography, however, is beyond the scope of the present paper.

To address whether ambient seismic noise is coherent over large distances across the Pacific we investigate the SNR of year-long cross-correlations observed at and between Pacific Ocean stations with and between stations located near the Pacific Rim. We concentrate on the period band between 10 sec and 150 sec where coherent ambient noise has been observed to exist on continents between distant stations. The study is based on ambient noise observed at 32 Pacific Ocean island stations, one ocean bottom installation (H2O), and 33 continental stations surrounding the Pacific Ocean (Fig. 1a).

Data

For all 12 months of the year 2003, we obtained the one sample per second long-period vertical component (LHZ) seismograms available from the IRIS Data Management Center for the stations shown in Figure 1a. Most of these data are from the GSN (Butler et al., 2004) or affiliated stations. Data are processed one day at a time. After removing the mean, daily trend and the instrument response, the data are filtered into four period bands: 10-25 sec, 33-67 sec, 50-100 sec, and 70-150 sec. In each band, the data are whitened in frequency and then amplitude normalized in time to suppress temporally localized events such as earthquakes and instrumental irregularities such as automatic mass re-centering. Cross-correlations between stations are computed daily and stacked over a year. The signal-to-noise ratio (SNR) is computed by comparing the peak amplitude of the signal in the group velocity windows defined by the global model of

Shapiro and Ritzwoller (2002) with the root-mean-square noise trailing the arrival window. (See Fig. 2.) This is done both at positive and negative correlation lag, corresponding to waves traveling in opposite directions between stations. Conclusions about the existence or absence of coherent noise between pairs of stations are made on the basis of the SNR. The SNR reported here is from the “symmetric signal”, the average of the cross-correlations with positive and negative lag, so that a single SNR is reported for each station pair. Cross-correlations between other components (e.g., radial-radial, vertical-radial, transverse-transverse) could also have been performed, but to establish the existence or absence of coherent noise, consideration of vertical-vertical cross-correlations is sufficient and preferable, in fact, due to the better SNR characteristics of the vertical component.

If the SNR > 10, the cross-correlation is considered to provide an estimated Green function for a wave traveling between the station pair. High SNR Green functions are observed in all frequency bands, as seen in Figure 2. In addition, high SNR Green functions are observed between island stations and island – continent pairs as shown in Figure 3a, which presents both the positive and negative lags of the cross-correlation.

To illuminate the results on the coherence of ambient noise between station pairs, we compare the observed SNR of the estimated Green functions with the level of local ambient noise at each station. The ambient noise level (ANL) is estimated using the method of Berger et al. (2004). The example cross-correlations shown in Figure 3a are contrasted with the ANL estimates of the stations presented in Figure 3b. Peterson's Standard Low Noise Model (SLNM) is shown for comparison (Peterson, 1993).

Results

The principal result of the paper appears in Figure 1b-d. In each of three period bands (the 50-100 sec band is not shown because of similarity to 33-67 sec), lines are drawn between station pairs with SNR > 10 on the symmetric component of the 12 month cross-correlation. These maps show that coherent noise exists between island-island station pairs (e.g., WAKE-MIDW at 10-25 sec), island-continent station pairs (e.g., POHA-WHY at 10-25 sec), and, consistent with earlier studies, continent-continent station pairs (e.g. LLLB-COR at 10-25 sec and many others). The number of station pairs with high SNR Green functions (SNR>10) increases with period: 120 from 10-25 sec, 212 from 33-67 sec, 215 from 50 -100 sec, and 298 from 70-150 sec. The longer periods are, not surprisingly, more coherent over greater distances. Scattering and anelastic attenuation act to de-correlate propagating wave-fields more strongly at the shorter period end of the spectrum.

Closer inspection of the SNR of cross-correlations between island-island station pairs reveals that atolls such as Wake and Kwajalein Islands are relatively unlikely to have coherent ambient noise observed with each other, with larger oceanic islands (e.g., Hawaii, Adak, Tahiti, American Samoa, etc.), or with continental stations. Ambient noise at large oceanic islands tends to cohere more strongly with other large islands or continental stations, as Figure 1b-d shows. This is consistent with the hypothesis that oceanic island stations suffer from locally generated noise which obscures the observation of the long-distance coherent wavefield which is the basis for ambient noise tomography. Noise conditions at atolls are more likely to be dominated by local noise as the stations cannot be isolated from the nearly direct effects of nearby wave action.

To test the hypothesis that local noise obscures the coherent noise observable between many station pairs, the ANL for each station is computed and compared with Peterson's Standard Low Noise Model (SLNM). The SLNM probably provides an upper bound on the long distance coherent noise level, and the difference between the ANL and SLNM derives predominantly from local noise. Figure 4a presents examples of cross-correlations between 33 and 67 sec period and Figure 4b shows ANLs for four stations near to Hawaii: POHA, KIP, MAUI, and H2O, located respectively on the Big Island of Hawaii, Oahu, Maui, and on the ocean bottom off-shore. The H2O station was installed on the retired Hawaii-2 ocean bottom co-axial telephone cable about 2000 km northeast of Oahu. Data flow stopped on May 23, 2003, so all cross-correlations with H2O are less than 5 months in duration. The ANL for H2O is similar to the ocean bottom curve of Webb (1998). The SNR of the cross-correlations (Fig. 4a) between these stations on or near Hawaii and the GSN station in Corvallis, OR (COR) is inversely related to the noise level at the stations between 33 and 67 sec period (Fig. 4b). The POHA station, for example, has the highest cross-correlation SNR and the lowest ANL. Higher ANLs for KIP, MAUI, and H2O reflect higher local noise that is incoherent with noise at distant stations and, therefore, does not contribute constructively to the cross-correlations. The traditional characteristics sought to site seismic stations for earthquake seismology, namely locally quiet conditions, are also essential to observe coherent noise signals over long distances.

As a closing note on the sub-oceanic borehole station H2O, Figure 1b shows that coherent ambient noise is observed between H2O and several other stations at periods from 10-25 sec. In this period range, the ANL for H2O is comparable to other stations, as Figure 4b demonstrates. At longer periods, however, local noise at H2O is higher, overcomes the background coherent noise, and vitiates the cross-correlation. Such long period local noise is probably caused by tilting under fluid flow and seafloor deformation under surface gravity waves which can raise deep seafloor vertical component noise by 35-40 db and 5-15 db, respectively (Webb and Crawford, 1999; Crawford et al., 2006) Crawford and Webb (2000) and Crawford et al. (2006) describe a method by which data from the horizontal seismometer channel and a co-located differential seafloor pressure gauge can be used to remove most of the tilt and deformation signal from the local noise. Crawford et al. (2006) argue that this step will be crucial for ambient noise tomography to be applied successfully to ocean bottom seismometers (OBS) at periods above about 20 sec.

Figure 5 further quantifies the relation between local noise level at the station and the coherence of ambient noise over long distances. For each station, we plot the ANL of the station versus the longest distance at which a high SNR cross-correlation signal is observed for that station, called the “noise coherence distance”. At periods larger than about 25 sec, there is a cut-off noise level of about -170db above which no high SNR cross-correlation is observed. In addition, the noise coherence distance increases if local noise decreases. This appears in Figure 5 as a trend that the lower the ANL the greater the distance at which high SNR Green functions can be observed. Above 20 sec period the inverse slope is about 1700 km/dB at 51 and 71 sec and about 2800 km/dB at 100 sec period. At 19 sec period, there is no distance trend, probably due to strong attenuation and scattering in this period band and the large inter-station distances considered in this study. The similar trends for island and continental stations indicate that there is no intrinsic difference between island and continental stations in terms of the relationship between ANL and noise coherence distance.

The symbols plotted at zero distance in Figure 5 are for stations that do not produce a high SNR on any cross-correlation. Among these, a few stations (XMAS, JOHN, HNR and DAV) with unusual ANLs probably suffer from instrumental problems. Others are mainly stations on atolls, the ocean bottom station H2O, and a few continental stations near the edges of our coverage where few inter-station cross-correlations are computed.

In conclusion, similar to continental paths, ambient seismic noise is coherent over long distances along oceanic paths. The physical foundation is established, on the basis of this coherent signal, for ambient noise tomography to be performed across the Pacific Basin and by implication across other oceanic basins. The practical requirement for retrieving useful Green functions from ambient noise is for the stations to be locally quiet or local noise to be removed or reduced in some fashion. Strong local noise obscures the coherent ambient noise observable between pairs of distant stations. The existence of strong local noise at many oceanic sites provides a major challenge for ambient noise tomography, particularly at atoll sites and at ocean bottom sites at long periods. The demonstration by Crawford et al. (2006) of the ability to use horizontal component seismometer data and seafloor pressure gauge data to correct vertical component seafloor data for local tilt and crustal deformation makes us optimistic that ambient noise tomography can be applied successfully to accruing ocean bottom seismic data.

Acknowledgments

The authors would like to thank two anonymous reviewers for constructive criticism, Spahr Webb for helpful discussions of the removal of tilt noise from ocean bottom vertical components, and Wayne Crawford for a preprint. All data used in this paper were obtained from the IRIS-DMC. This work has been supported by NSF grant EAR-0409217.

References

Berger, J., P. Davis, and G. Ekstrom, Ambient Earth noise: A survey of the Global Seismic Network, *J. Geophys. Res.*, 109, B11307, doi:10.1029/2004JB003408, 2004.

Butler, R. T. Lay, K. Creager, P. Earl, K. Fischer, J. Gaherty, G. Laske, B. Leith, J. Park, M. Ritzwoller, J. Tromp, and L. Wen, The global seismic network surpasses its design goal, *EOS,* 85(23), 8 June 2004.

Crawford, W.C., and S.C. Webb, Identifying and removing tilt noise from low-frequency (<0.1 Hz) seafloor vertical seismic data, *Bull. Seism. Soc. Amer.*, 90, 952-963, 2000.

Crawford, W.C., R.A. Stephen, and S.T. Bolmer, A second look at low-frequency marine vertical seismometer data quality at the OSN-1 site off of Hawaii for seafloor, buried and borehole emplacements, submitted, 2006.

Peterson, J. Observations and modeling of seismic background noise, *Open-File Report*, 93-322, US Geological Survey, Albuquerque, NM, 1993.

Sabra, K.G., P. Gerstoft, P. Roux, W.A.Kuperman, and M.C. Fehler, Surface wave tomography from microseisms in Southern California, *Geophys. Res. Lett.*, 32, doi:10.1029/2005GL023155, 2005.

Shapiro, N.M. and M.H. Ritzwoller, Monte-Carlo inversion for a global shear velocity model of the crust and upper mantle, *Geophys. J. Int.*, 151, 88-105, 2002.

Shapiro, N.M. and M. Campillo, Emergence of broadband Rayleigh waves from correlations of the ambient noise, *Geophys. Res. Lett.*, 31, doi:10.1029/2004GL019491, 2004.

Shapiro, N.M., M. Campillo, L. Stehy, and M.H. Ritzwoller, High-resolution surface wave tomography from ambient seismic noise, *Science*, 307, 1615-1618, 2005.

Webb, S.C., Broadband seismology and noise under the ocean, *Revs. Geophys.*, 36, 105-142, 1998.

Webb, S.C., and W.C. Crawford, Long-period seafloor seismology and deformation under ocean waves, *Bull. Seism. Soc. Amer.*, 89, 1535-1542, 1999.

Figure Captions

Figure 1. (a) Stations used in this study. (QSPA near the South Pole does not show on this projection). (b) – (d) Lines link stations whose year-long cross-correlations have a SNR > 10. (b) 10s to 25s period. (c) 33s to 67s. (d) 70s to 150s.

Figure 2. Example year long broad-band symmetric component cross-correlations between two island stations: RPN (Rapanui, Easter Island) and PPT (Papeete, Tahiti). Grey shaded regions mark the group arrival window predicted by the 3-D model of Shapiro and Ritzwoller (2002), expanded by 75 sec in both directions. The SNR is defined as the peak amplitude in the window divided by the rms of the trailing noise. The period band and SNR are identified in each panel.

Figure 3. (a) Year-long cross-correlations between station pairs between periods of 70 and 150 sec. From top to bottom: continent station (COLA, College, AK) – continent

station (PFO, Pinyon Flat, CA); ocean island station (KIP, Kipapa, Oahu, HI) – continent station (PFO); ocean island station (AFI, Afiamalu, Samoa Is.) – ocean island station (KIP). The SNR is reported for the symmetric component. (b) Ambient noise level (ANL) computed for the stations COLA, PFO, KIP, and AFI compared with Peterson's Standard Low Noise Model (SLNM).

Figure 4. (a) Year-long 33-67s period cross-correlations between station COR, Corvallis Oregon, and four stations near to or on Hawaii (KIP, Kipapa, Oahu, HI; MAUI, Maui, HI; POHA, Big Island of Hawaii; H2O, ocean bottom borehole stations about 2000 km northeast of Oahu). The SNR on the symmetric signal is indicated on each graph. (b) Ambient noise level (ANL) computed for the stations KIP, POHA, MAUI, and H2O compared with Peterson's Standard Low Noise Model (SLNM). The 33s to 67s window is shown on the graph.

Figure 5. The ambient noise level (ANL) of each station plotted versus the longest distance at which a high SNR cross-correlation signal is observed for that station. (a) 100 sec period. (b) 71 sec, (c) 51 sec, and (d) 19 sec. The best fit line is calculated using all

nonzero distance points. Symbol types discriminate between continent and ocean stations (including station H2O). Names of some noisy stations and the stations with likely instrumental problem are listed on the graphs.

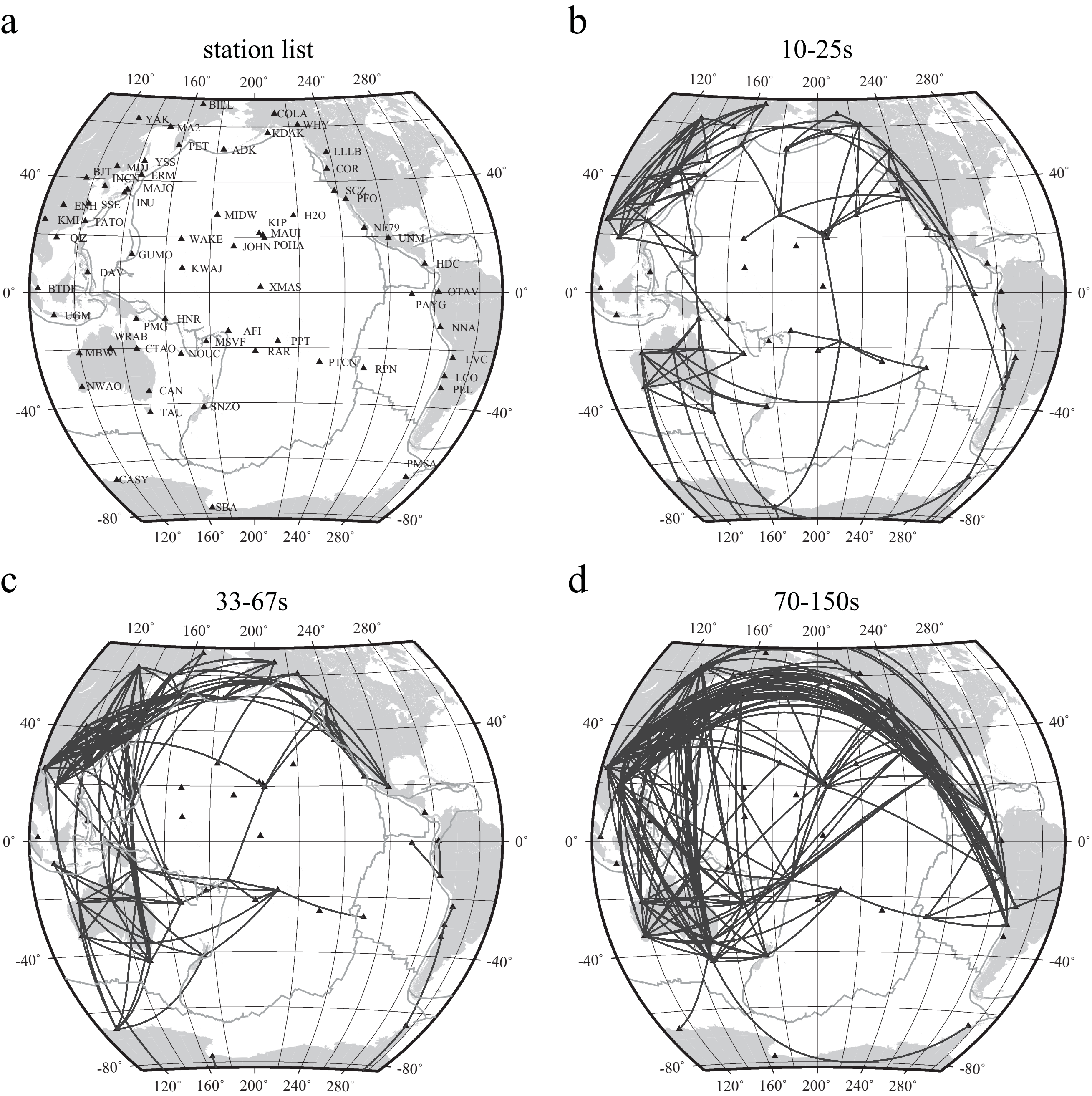
a
station list
b
10-25s
c
33-67s
d
70-150s
120°
160°
200°
240°
280°
40°
0°
-40°
-80°
BILL
YAK
MA2
COLA
WHY
KDAK
PET
ADK
LLLB
COR
YSS
MDJ
BJT
ERM
INCN
MAJO
SCZ
PFO
INU
ENH
SSE
KMI
TATO
MIDW
H2O
KIP
MAUI
POHA
NE79
UNM
QIZ
WAKE
JOHN
GUMO
KWAJ
HDC
DAV
XMAS
BTDF
OTAV
PAYG
UGM
HNR
PMG
AFI
NNA
WRAB
PPT
MSVF
MBWA
CTAO
NOUC
RAR
LVC
PTCN
RPN
LCO
NWAO
CAN
PEL
SNZO
TAU
PMSA
CASY
SBA

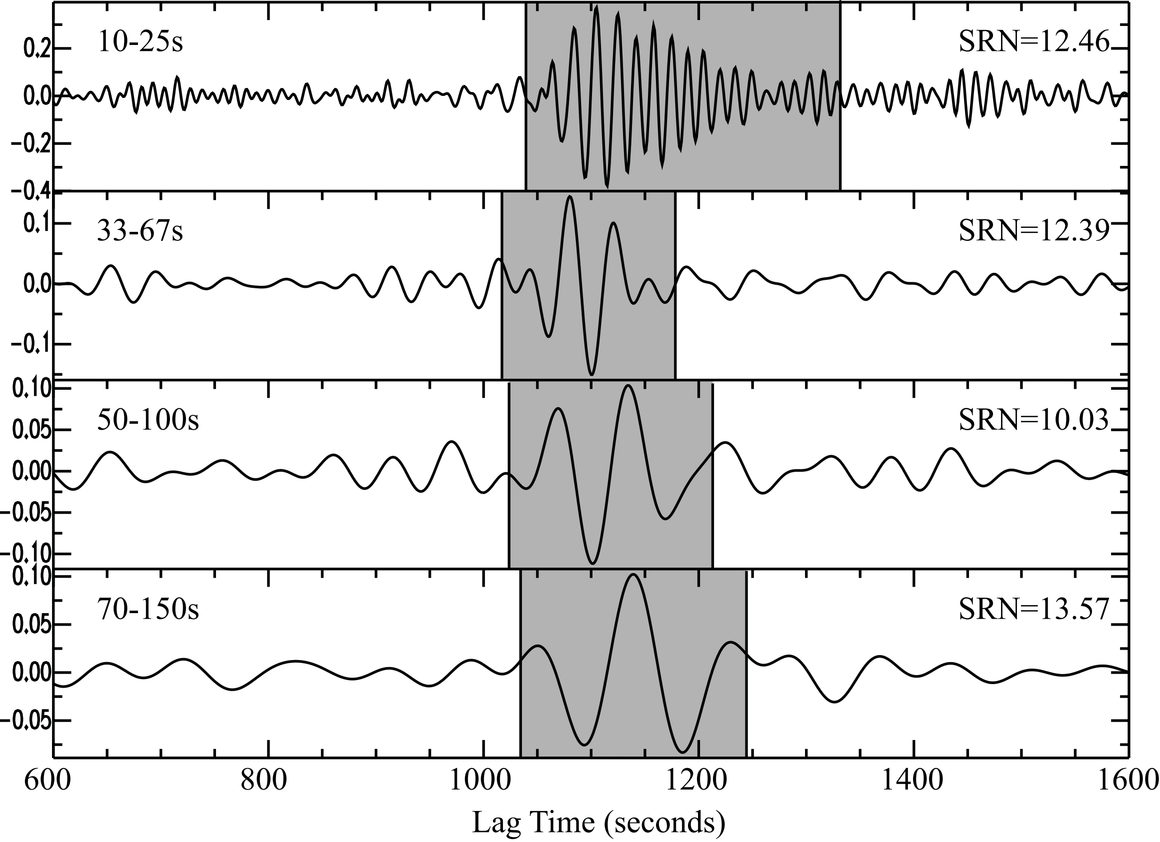
10-25s
SRN=12.46
0.2
0.0
-0.2
-0.4
33-67s
SRN=12.39
0.1
0.0
-0.1
50-100s
SRN=10.03
0.10
0.05
0.00
-0.05
-0.10
70-150s
SRN=13.57
0.10
0.05
0.00
-0.05
600
800
1000
1200
1400
1600
Lag Time (seconds)

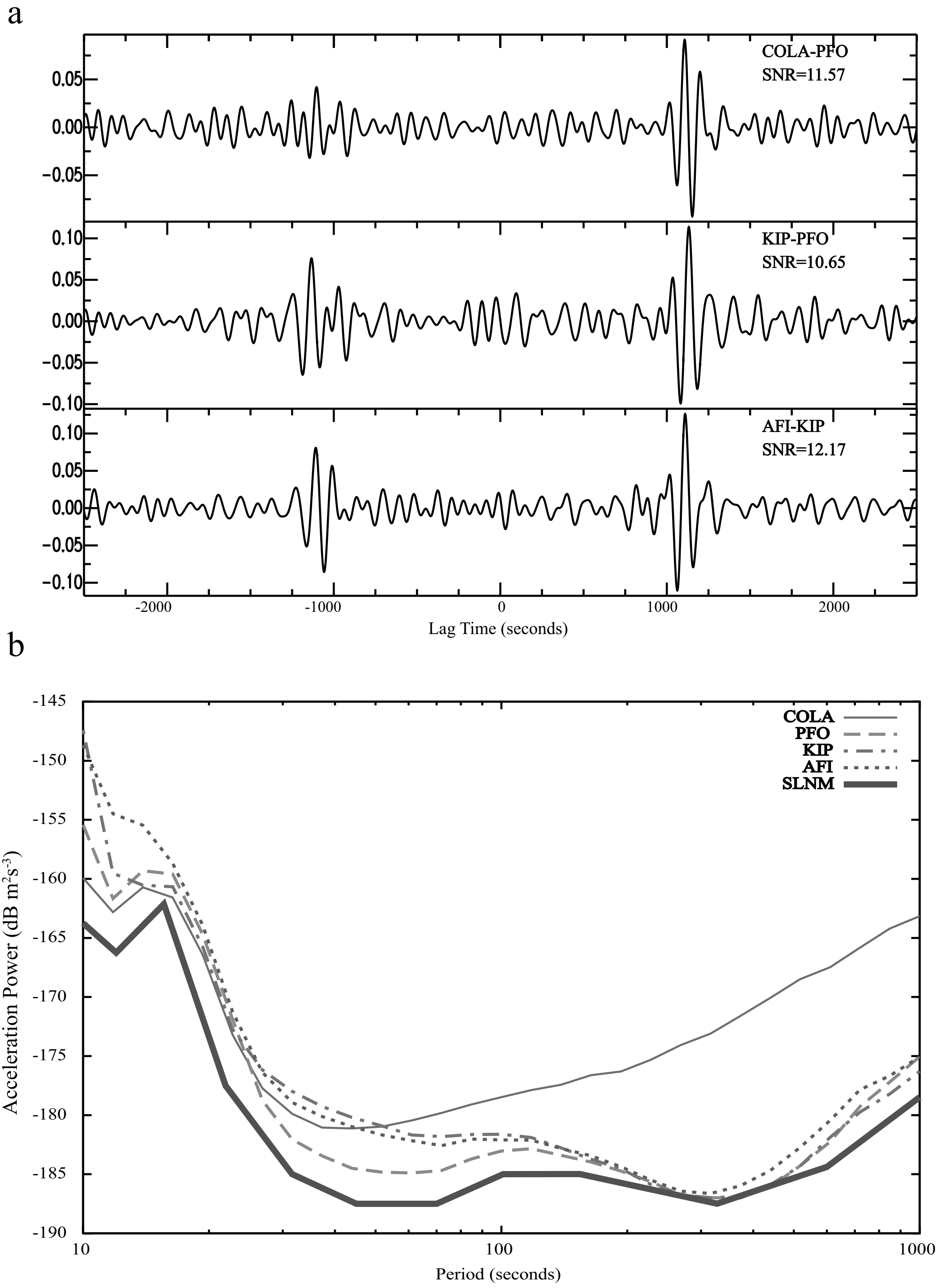
a
COLA-PFO
SNR=11.57
KIP-PFO
SNR=10.65
AFI-KIP
SNR=12.17
0.10
0.05
0.00
−0.05
−0.10
-2000
-1000
0
1000
2000
Lag Time (seconds)
b
COLA
PFO
KIP
AFI
SLNM
-145
-150
-155
-160
-165
-170
-175
-180
-185
-190
Acceleration Power (dB m^{2}s^{-3})
10
100
1000
Period (seconds)

a

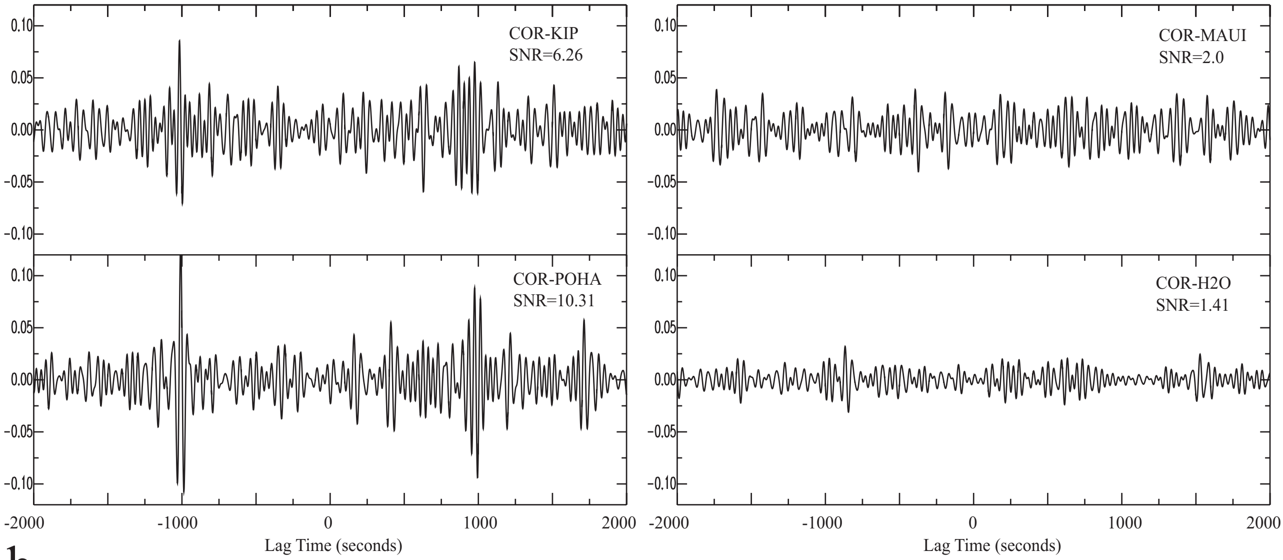
COR-KIP
SNR=6.26
COR-MAUI
SNR=2.0
COR-POHA
SNR=10.31
COR-H2O
SNR=1.41
0.10
0.05
0.00
−0.05
−0.10
-2000
-1000
0
1000
2000
Lag Time (seconds)

b

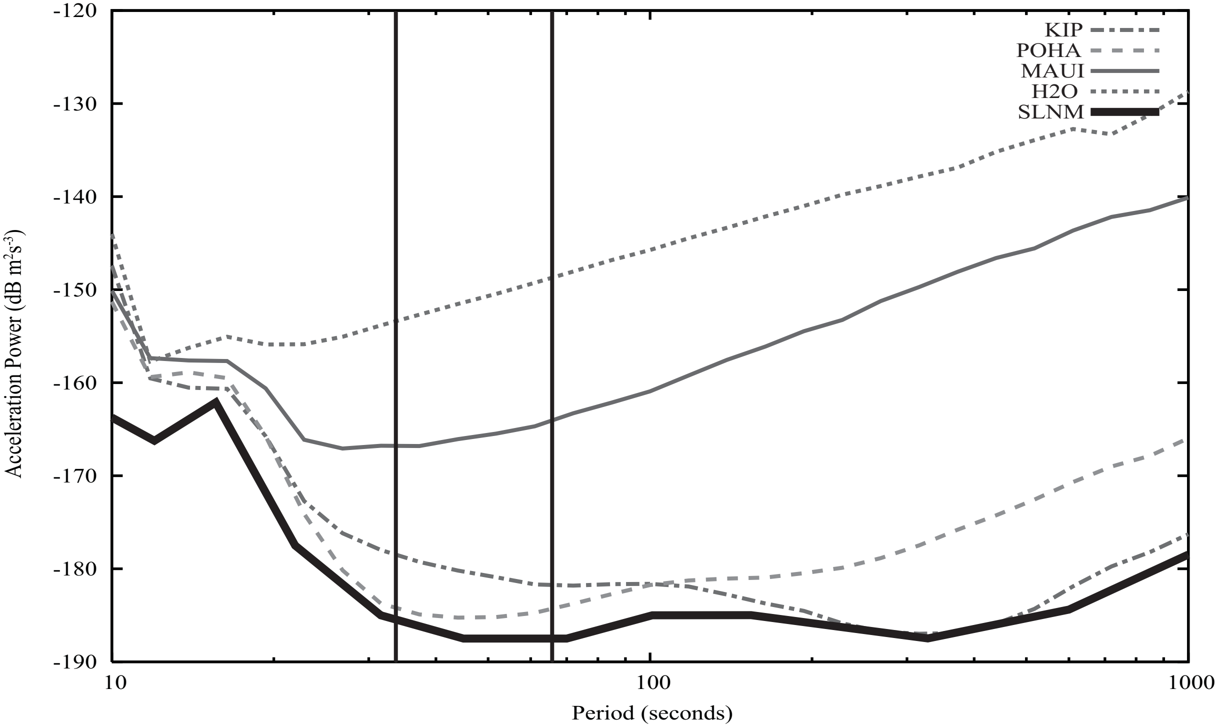
KIP
POHA
MAUI
H2O
SLNM
-120
-130
-140
-150
-160
-170
-180
-190
Acceleration Power (dB m^2s^{-3})
10
100
1000
Period (seconds)

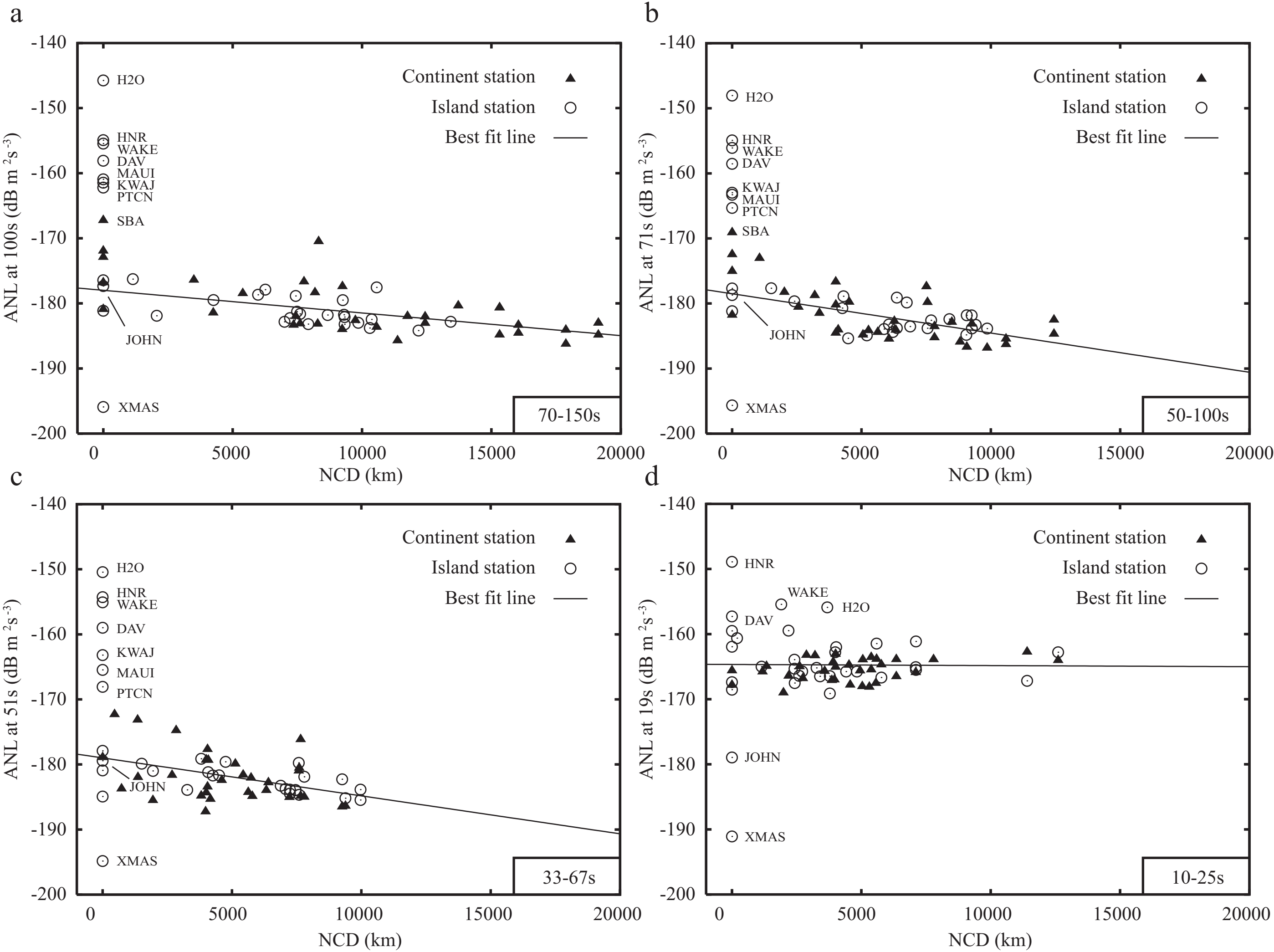
a
b
c
d
ANL at 100s (dB m ^{2}s $^{-3}$)
ANL at 71s (dB m ^{2}s $^{-3}$)
ANL at 51s (dB m ^{2}s $^{-3}$)
ANL at 19s (dB m ^{2}s $^{-3}$)
NCD (km)
-140
-150
-160
-170
-180
-190
-200
0
5000
10000
15000
20000
Continent station
Island station
Best fit line
H2O
HNR
WAKE
DAV
MAUI
KWAJ
PTCN
SBA
JOHN
XMAS
70-150s
50-100s
33-67s
10-25s